Experiments with individual spins, using the diamond NV-centre

Diamond has a number of well characterized defects, of which the most prominent one is the nitrogen-vacancy center [1, 2, 3]. It consists of a nitrogen at a carbon site and an adjacent vacancy, i.e. a missing carbon. The electrons of the defect combine to an $S = 1$ total spin. The attractive properties of this center include the long coherence times at room temperature, and the special optical properties: the photostability is very high, allowing experiments on single centers for months.

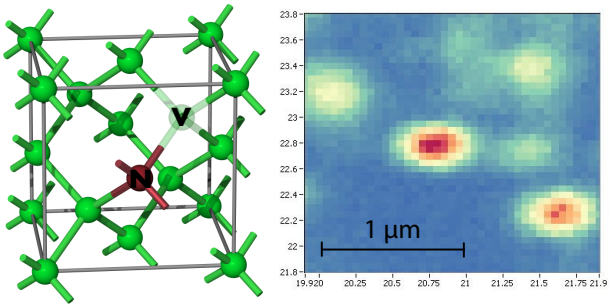

Figure 1: Structure of the N/V center in diamond. The right-hand side represents an image of a diamond surface, recorded by a scanning confocal microscope. Each bright spot represents a single N/V center.

Each of the bright spots in the right-hand part of Fig. 1 represents a single N/V center. While it is not possible to determine this from the image alone, which was taken by scanning confocal microscopy with a resolution of $\approx$ 300 nm, it is possible to estimate it from the observed count rate. A much cleaner signature is obtained by measuring the correlation function of the arrival times of the photons on the detector. If we measure the delays τ between the arrival times of individual photons, we find that the probability to detect a second photon immediately after the first drops to zero for short times [4]. This is easy to understand by considering that after the emission of a photon, the center is in the ground state and cannot emit another photon until it has absorbed one.

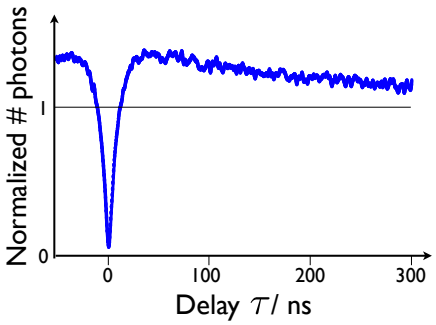

Figure 2: Photon correlation function for a single N/V center.

Fig. 2 shows an example: the emission rate drops almost to zero for short delays, and it takes $\approx$ 15 ns for the emission probability to rise again to its average value. This rise time decreases with increasing laser intensity.

Initialization as well as readout rely on absorption-emission cycles between the $^3A_2$ electronic ground state and the ^3E electronically excited state, whose zero phoonon line has a wavelength of $\lambda_0 = 637\,\text{nm}$. The phonon sidebands can be excited by green laser light (e.g. $\lambda = 532\,\text{nm}$). Between these two electronic triplet states are two singlet states, which can be populated by intersystem crossing processes. These processes are spin dependent. Pumping the system for $\approx 0.5\,\mu$s with 1 mW of green laser light leaves it with high probability in the $m_S = 0$ spin state. When the system is in the $m_S = 0$ state, the scattering rate for unpolarized green light is about twice that of the $m_S = \pm 1$ states, which allows a relatively straightforward detection of the individual spin states.

In the absense of a magnetic field, the $m_S = \pm 1$ spin states are degenerate, but separated from the $m_S = 0$ state by the zero field splitting of $D = 2.87$ GHz. A magnetic field lifts the degeneracy of the $m_S = \pm 1$ states. In addition, the electron spin is coupled to the nitrogen nuclear spin (usually ^{14}N, $I = 1$) and to a those carbon sites that are occupied by a ^{13}C isotope ($I = 1/2$) with a hyperfine coupling constant that starts at 130 MHz for the carbon sites adjacent to the vacancy and decreases with the distance [5]. The most important terms in the ground-state Hamiltonian of the NV defect are therefore

$$\mathcal{H} = D\,S_z^2 + \mu_0 g \vec{B}\vec{S} + A_N \vec{S}\vec{I}_N + \sum_k A_C^k \vec{S}\vec{I}_C^k,$$

where the sum runs over all sites occupied by ^{13}C isotopes.

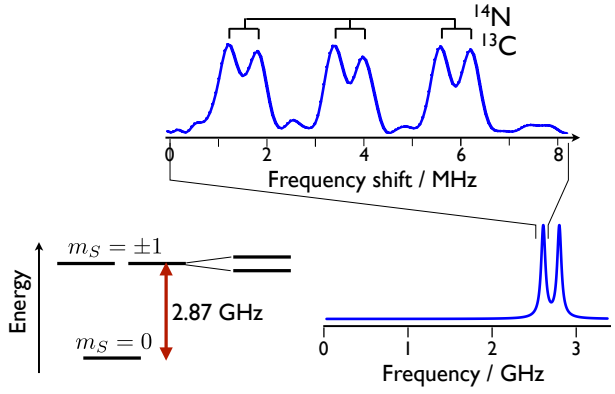

Figure 3: Spectrum from a single N/V center showing resolved hyperfine couplings to the ^{14}N and one ^{13}C nuclear spin.

Figure 3 shows a typical spectrum: the $m_S = 0 \rightarrow m_S = -1$ transition of the electron spin is split by the hyperfine interaction with the ^{14}N nuclear spin ($A_N = 2.17$ MHz) and one ^{13}C nuclear spin ($A_C = 0.58$ MHz). Many additional nuclear spins couple to the

electron spin with hyperfine coupling constants ≤ 0.3 MHz, which do not lead to resolved splittings, but to a broadening of the resonance line.

The NV center is a very interesting system for the implementation of quantum bits (qubits) [6, 7, 3] in solid-state systems: it allow relatively easy detection of individual spins, is highly stable, can be operated at room temperature, and it is scalable, in the sense that large numbers of NV centers can be placed in a single diamond crystal. Nevertheless, a number of issues have to be addressed, before a large-scale quantum computer on the basis of individual NV-centers becomes a reality. On the material side, this includes the preparation of sufficiently pure samples, to avoid perturbations by magnetic defects and the controlled implantation of nitrogen atoms to generate N/V defects at the appropriate locations. On the side of the spin physics, we work on extending the lifetime of the qubits by a suitable choice of parameters, as well as by active protection schemes like dynamical decoupling.

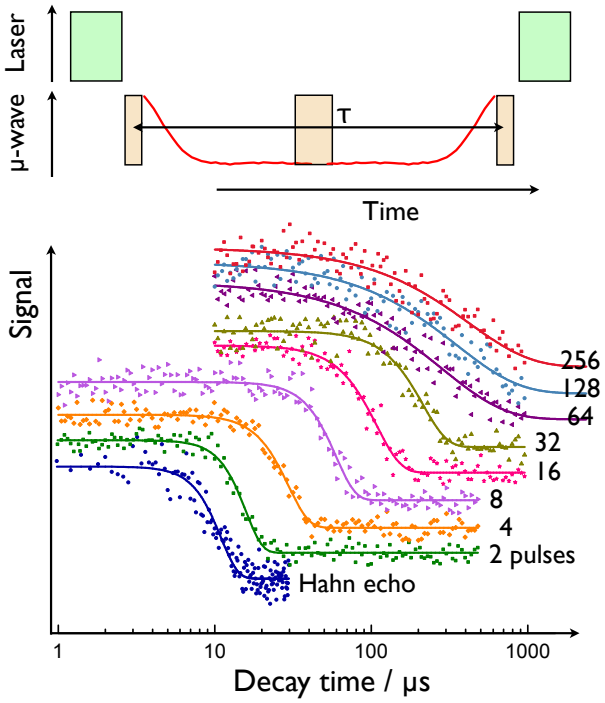

Figure 4: Refocusing of electron spin coherence by spin-echo experiments. The curves in the lower panel show the decay of the echo amplitude as a function of the total measurement time for different experiments with increasing number of refocusing pulses [8].

The decay of electron spin coherence by the hyperfine interaction with the ^{13}C nuclear spins can be refocused by the usual spin-echo experiments. As shown in Fig. 4, a single refocusing pulse, corresponding to the Hahn echo, can generate echoes for delays of up to 10 μs. For longer times, the refocusing does not work, because fluctuations in the environment make the refocusing inefficient. Like in the case of molecular diffusion, it becomes then necessary to apply multiple refocusing pulses with shorter delays between them [9, 10, 11, 12, 13]. As shown by the other curves in Fig. 4, sequences of refocusing pulses can extend the coherence time up to >2 ms [8].

Simultaneously, we work on the implementation of quantum logical gate operations with high fidelity. This requires precise knowledge of the system Hamiltonian (e.g. zero field splitting, orientation of the symmetry axis of the center). In addition, we have to design the gate operations in such a way that their overall effect matches closely the ideal target operation, even if the experimental parameters (e.g. amplitude of control field) differs from the ideal target value.

References

[1] M. W. Doherty, N. B. Manson, P. Delaney, and L. C. L. Hollenberg, New J. Phys. **13**, 025019 (2011).

[2] F. Jelezko and J. Wrachtrup, physica status solidi (a) **203**, 3207 (2006).

[3] D. Suter and F. Jelezko, Progress in Nuclear Magnetic Resonance Spectroscopy **98-99**, 50 (2017), ISSN 0079-6565.

[4] H. Kimble, M. Dagenais, and L. Mandel, Phys. Rev. Lett. **39**, 691 (1977).

[5] B. Smeltzer, L. Childress, and A. Gali, New Journal of Physics **13**, 025021 (2011).

[6] M. A. Nielsen and I. L. Chuang, *Quantum computation and quantum information* (Cambridge Univ. Press, Cambridge, 2001).

[7] J. Stolze and D. Suter, *Quantum Computing: A Short Course from Theory to Experiment* (Wiley-VCH, Berlin, 2008), 2nd ed., ISBN 978-3-527-40787-3.

[8] J. H. Shim, I. Niemeyer, J. Zhang, and D. Suter, Europhys. Lett. **99**, 40004 (2012).

[9] H. Carr and E. Purcell, Phys. Rev. **94**, 630 (1954).

[10] S. Meiboom and D. Gill, Review of Scientific Instruments **29**, 688 (1958).

[11] A. M. Souza, G. A. Álvarez, and D. Suter, Phys. Rev. Lett. **106**, 240501 (2011).

[12] A. M. Souza, G. A. Álvarez, and D. Suter, Phil. Trans. R. Soc. Lond. A **370**, 4748 (2012).

[13] D. Suter and G. A. Álvarez, Rev. Mod. Phys. **88**, 041001 (2016).